International Journal of
Drug Discovery and Pharmacology（IJDDP）

Scilight

Article

Eupatorium Lindleyanum DC. Extract Protects against MPTP-induced Mouse of Parkinson's Disease by Targeting Neuroinflammation

Yichi Zhang [1], Lu Yao [1], Xiaowen Zhang [1], Zhuo Yang [1], Yang Chen [2], Lingli Zheng [1], Yongzhe Zheng [1], Wei Yu [2], Nilufar Z. Mamadalieva [3], Bo Han [2], Pengfei Tu [1], Rimma F. Mukhamatkhanova [3], and Kewu Zeng [1,*]

[1] State Key Laboratory of Natural and Biomimetic Drugs, School of Pharmaceutical Sciences, Peking University, Beijing 100191, China
[2] School of Pharmacy/Key Laboratory of Xinjiang Phytomedicine Resource and Utilization, Shihezi University, Shihezi 832003, China
[3] Institute of the Chemistry of Plant Substances AS RUz, Mirzo Ulugbek Str 77, Tashkent 100170, Uzbekistan
* Correspondence: ZKW@bjmu.edu.cn

Received: 10 May 2024; Revised: 14 May 2024; Accepted: 24 May 2024; Published: 6 June 2024

Abstract: Background: Neuroinflammation plays a vital role in the pathology of Parkinson's disease (PD). *Eupatorium lindleyanum* DC. (EL) has previously reported to exert anti-inflammation activity. Methods: In the present study, we examined the effects of the EL extract (ELE) on 1-methyl-4-phenyl-1, 2, 3, 6-tetrahydropyridine (MPTP)-induced mouse model of PD and potential molecular mechanisms. The anti-neuroinflammation effect of ELE was also determined in lipopolysaccharide (LPS)-induced BV-2 cells in vitro. Moreover, the ELE-interacting target proteins were identified. And the bioinformatics analysis was performed based on the identified targets. Results: Our results showed that ELE significantly alleviated motor performance impairment and neuronal damage in MPTP-induced PD mice. In particular, ELE reversed MPTP-induced neuroinflammation via inhibiting microglial activation that was associated with progressive PD. Moreover, the anti-neuroinflammation effect of ELE was confirmed in LPS-induced BV-2 cells by detecting the release of pro-inflammatory factors such as nitric oxide (NO), interleukin-6 (Il-6), tumor necrosis factor-α (TNF-α), inducible nitric oxide synthase (iNOS) and cyclooxygenase-2 (COX-2). Furthermore, the ELE- interacting target proteins were identified by affinity purification-mass spectrometry-based proteomics strategy. Then, AMP-activated protein kinase (AMPK) signaling pathway was enriched by kyoto encyclopedia of genes and genomes (KEGG) analysis. We found that ELE markedly increased AMPK phosphorylation and inhibited nuclear factor-κB (NF-κB) signal in BV-2 cells. Conclusion: Collectively, these results indicate that ELE may exert significant neuroprotective effects against PD via targeting neuroinflammation.

Keywords: Parkinson's disease; Neuroinflammation; *Eupatorium lindleyanum* DC.; Target identification; AMPK pathway

1. Introduction

Parkinson's disease (PD) is a neurodegenerative disease which is characterized by the progressive degeneration and loss of dopaminergic neurons in the substantia nigra [1–3]. The pathological mechanisms of PD is still largely unknown, resulting in the serious lack of effective treatments [4–6]. Neuroinflammation plays a central role in the pathology of PD [7,8]. Currently, neuroinflammation involves the excessive microglial activation and the consequent release of pro-inflammatory mediators [9,10]. Thus, microglial

activation is widely involved in PD pathology, particularly for dopamine (DA) neuron degeneration through the production of harmful substances such as pro-inflammatory mediators and reactive oxidative and nitrogen species [11,12]. Inhibition of microglial activation may aid in the treatment of PD. Therefore, anti-neuroinflammation is one of the promising strategies for PD [8].

The plant *Eupatorium lindleyanum* DC. (EL) has been demonstrated to have anti-hypertensive and anti-inflammatory activities [13]. As a traditional Chinese medicine, EL has the functions of resolving phlegm, suppressing cough, and relieving asthma [14]. It has been reported that EL shows protective effects on oleic acid-induced acute lung injury in rat [13]. Moreover, EL syrup is also used to treat cough, phlegm and chronic bronchitis [15]. Currently, more than 100 components have been isolated from this herb [16]. Among them, terpenoids are considered as the most important biological active substances [16]. Although the health benefits and promising anti-inflammation potential of EL have been increasingly recognized, the anti-PD activity of EL has not been investigated until now.

Since the development of PD is highly associated with neuroinflammation progress, in the present study, we tested the effects of the EL extract (ELE) on the PD mouse model induced by MPTP injection. The results showed that ELE significantly ameliorated the motor performance impairment and rescued dopaminergic neurons in MPTP-induced PD mice. Furthermore, ELE attenuated the MPTP-mediated neuroinflammation via suppressing the activation of microglia. Meanwhile, ELE dose-dependently suppressed LPS- induced BV-2 microglial activation via AMPK/mTOR/NF-κB signaling pathway. The activation of AMPK was known to exert anti-inflammatory effects. Activation of AMPK and subsequent inhibition of mTOR (mammalian target of rapamycin) reduced the activation of the NF-κB signaling pathway. Therefore, the regulation of AMPK/mTOR/NF- κB signaling pathway could inhibit microglial activation and reduce the neuroinflammation, which may contribute to PD treatment. Collectively, these observations suggest that ELE may exert neuroprotective effects against PD via targeting neuroinflammation. Thus, ELE may represent as a promising novel agent against PD.

2. Materials and Methods

2.1. Materials

MPTP was purchased from TargetMol (Shanghai, China). DMEM (high glucose), penicillin-streptomycin and trypsin were purchased from Macgene (Beijing, China). Fetal bovine serum (Excellent) was purchased from Shanghai NOVA Medical Science and Technology (Shanghai, China). MTTand LPS were purchased from Sigma-Aldrich (St. Louis, MO, USA). The NO detection kit was purchased from Nanjing Jiancheng Bioengineering Institute (Nanjing, Jiangsu, China) [17]. The crystal violet staining solution was purchased from Beyotime Biotechnology (Nanjing, Jiangsu, China). The IL-6 and TNF-α ELISA kits were purchased from ExCell Biotech (Taicang, Jiangsu, China) [17]. The Easy II protein quantitative kit (BCA) was purchased from TransGen (Beijing, China) [17]. The polyvinylidene fluoride (PVDF) microporous membrane was purchased from Merck KGaA (Darmstadt, Germany). The primary antibodies and secondary antibodies were purchased from Cell Signaling Technology (Beverly, MA, USA). Super enhanced chemiluminescence (ECL) substrate was purchased from Biodragon (Suzhou, Jiangsu, China). The PV-9000 two-step immunohistochemical staining kit was purchased from ZSGB-BIO (Beijing, China) [18].

2.2. Preparation of ELE

The plant EL was acquired from Kunming Zhifen Biotechnology company from Yunnan, China. The company conducted the authentication of the plant material. The plants were dried and powdered. The powdered plants were then reflux extracted with 95% EtOH for 1 h at 25 °C. The procedure was repeated for 3 times to extract the active compounds from the plant material. The liquor was filtered. Then, the filtered liquor was subsequently concentrated under reduced pressure to form solid powder.

2.3. Cell Culture

Mouse microglia BV-2 cell line and rat pheochromocytoma PC12 cell line were obtained from the Cell

Resource Center, Peking Union Medical College. The cells were cultured in DMEM supplemented with 10% inactivated fetal bovine serum (FBS), 100 U/mL penicillin and 100 μg/mL streptomycin at 37 °C in a cell incubator with 5% CO2. The status of the cells was monitored throughout the experiments to ensure their viability and functionality.

2.4. PC12 Cell Culture with Conditioned Medium (CM)

BV-2 cells were treated with ELE (12.5, 25, and 50 μg/mL) for 6 h. The dose of ELE was chosen according to our previous experiment. After removal of the medium, the cells were treated with LPS (1 μg/mL) for 24 h to collect CM. PC12 cells were cultured in the presence of CM for 24 h.

2.5. Cell Viability Assay

BV-2 cells were treated with LPS (1 μg/mL) with different concentrations of ELE (12.5, 25, and 50 μg/mL) for 24 h. After treatment, the medium was removed and the MTT solution (0.5 mg/mL) was added. The cells were incubated with MTT for 4 h at 37 °C to form formazan crystals. Dimethyl sulfoxide (DMSO) was added and the absorbance at 570 nm was detected with a microplate reader (Sunrise-Basic, TECAN, Männedorf, Switzerland).

2.6. Crystal Violet Staining Assay

BV-2 cells were treated with 4% paraformaldehyde for 30 min at 25 °C. After washes, the crystal violet staining solution was added and incubated for 20 min at 25 °C. After incubation, the images were taken with a fluorescence microscope (IX73, Olympus, Tokyo, Japan).

2.7. Nitrite Oxide (NO) Assay

BV-2 cells were treated with LPS (1 μg/mL) with different concentrations of ELE (12.5, 25, and 50 μg/mL) for 24 h. After treatment, the cell supernatant was collected and the production of NO was quantified by NO detection kit. The cell supernatant was mixed with Griess reagent. After incubation for 15 min at 25 °C, the absorbance at 570 nm was detected with a microplate reader.

2.8. Enzyme-Linked Immunosorbent Assay (ELISA)

BV-2 cells were treated with LPS (1 μg/mL) with different concentrations of ELE (12.5, 25, and 50 μg/mL) for 4 h (TNF-α) and 8 h (IL-6). After treatment, the cell supernatant was collected for pro-inflammatory cytokines analysis using commercial ELISA kits. The cell supernatant samples and biotin-conjugate was added to the ELISA microwell plate and incubated for 2 h at 25 °C. Then, streptavidin-HRP was added to the plate and incubated for 1 h at 25 °C in the plate. After incubation, the streptavidin-HRP was removed. Then, substrate solution was added to the plate and incubated for 15 min at 25 °C in dark. Stop solution was added to stop the reaction, and the absorbance at 450 nm was detected immediately with a microplate reader.

2.9. Western Blotting

After treatment, the cells were collected. For mouse brain samples, the brains were immediately removed after euthanasia and stored at −80 °C. Then, the samples were lysed by cold RIPA with phenylmethylsulfonylfluoride (PMSF) for 20 min. The *Easy* II protein quantitative kit (BCA) was used to detect the protein concentrations. Then, the protein samples were heated for 15 min at 98 °C with loading buffer, followed by SDS-PAGE separation. The proteins were subsequently transferred to PVDF membranes. The membranes were then blocked with 5% skimmed milk for 30 min at 25 °C. After that, the membranes were incubated with primary antibodies at 4 °C overnight. After incubation, the membranes were washed with TBS with Tween 20 (TBST) and then incubated with HRP-conjugated secondary antibodies for 1 h at 25 °C. The membranes were developed with enhanced chemiluminescence (ECL). Then, the membranes were scanned on Tanon 5200 Multi Chemiluminescent Imaging Analysis System (Tanon, Shanghai, China).

2.10. Affinity Purification for Target Identification

The target proteins of ELE were identified by affinity purification strategy (pulldown) according to previously reported methods with slight modifications [19]. 4, 4'-dihydroxybenzophenone (DHBP)-bound Fe_3O_4 nanoparticles (NPs) reacted with ELE under ultraviolet radiation to generate ELE-crosslinked NPs (ELE beads). The ELE beads were then incubated with BV-2 cell lysates at 4 °C overnight to capture the target proteins.

2.11. Mass Spectrometry Analysis

To identify the bead-captured proteins, the nano LC-MS/MS experiment was carried out using Thermo Scientific EASY-nLC II system (ThermoFisher Scientific, Waltham, MA, USA) and a nano-HPLC-tandem LTQ Orbitrap Velos Pro mass spectrometer (LTQ-Orbitrap, Thermo Fisher Scientific, Waltham, MA, USA). The SEQUEST search engine (Thermo Fisher Scientific, Waltham, MA, USA) and Proteome Discoverer (1.4) software were used to analyze the tandem mass spectrometry data. The valuable simple peptide sequences detected were retrieved by UniProt.

2.12. Experimental Animals

Male C57BL/6J mice (6 weeks, 18 – 20 g) were purchased from Department of Laboratory Animal Science, Peking University Health Science Center. All procedures were approved by the Institutional Animal Care and Use Committee of Peking University (license no. LA2023010).

2.13. Parkinson's Model Mice (PD mice)

PD model was established according to previously reported methods with slight modifications [20]. As the previous report, the natural-derived small molecule eupalinolide B (EB) from EL was treated in mice with 50 mg/kg and exerted neuroprotective effects on PD pathology [20]. Given the composition of EB in ELE, we focused on evaluating the anti-PD activity by administering doses of 100 and 400 mg/kg ELE. The mice were divided into 4 groups (n=5 for each group), including control group, Parkinson's model group and ELE (100 and 400 mg/kg) treatment groups. Saline (vehicle) or ELE (100 or 400 mg/kg) was given for 15 days during the whole experiment. Daily treatment was started 10 days before MPTP administration. To establish PD model, the mice were injected intraperitoneally with MPTP solution (30 mg/kg) per day for 5 days. Saline was given to the control group as vehicle. The formal behavioral experiments were carried out at the fifth day.

2.14. Behavioral Evaluation

Behavioral evaluation was carried out according to the previously reported methods with slight modifications [20–22].

Rotarod test: The mice were gently placed on a rotarod apparatus (YLS-4C, Yiyan Scientific Research, Jinan, Shandong, China) at a rotational speed of 30 rpm. The mice safely fell off the rod when exhausted, and the latency of the mice before falling off in 180 s was recorded. The mice were given trials for pretraining before the formal experiment.

Pole test: The mice were gently placed at the top of a wooden inclined pole system (YLS-Q15, Yiyan Scientific Research, Jinan, Shandong, China). The time for climbing down the pole was recorded. The mice were given 3 trials for pretraining before the formal experiment.

Grip strength test: The grip strength of mice was measured with an automated grip strength meter (YLS-13A, Yiyan Scientific Research, Jinan, Shandong, China). The mice were grasped gently at the base of the tail and led to grip the apparatus. Then the mice were horizontally pulled away gently, and the peak grip strength was recorded. The test was repeated 3 times to evaluate the average.

Gait analysis: The gait of mice was analyzed with the VisuGait gait analysis system (XR-XFP101, Xinruan Information Technology, Shanghai, China). The gait analysis system consisted of a hardware system of an enclosed walkway on a glass plate and a high-speed video camera. Green light entered at the edge of the plate and was completely reflected except at the areas being touched. Mice were allowed to traverse the glass

walkway from one side to the other in an unforced manner. Paws were digitally captured by the video camera that was placed underneath the walkway. The gait analysis system included a software package for assessment. Quantitative analysis of the data from the VisuGait gait analysis system included the following parameters:

Stride length: The distance between two consecutive footprints of the left front paw.

Body speed: The ratio of total walk length to time of finishing an entire walk.

Normal step sequence: The percentage of normal step sequence patterns in an entire walk.

2.15. Immunohistochemical (IHC) Assay

After behavioral evaluation, the mice were euthanized by cervical dislocation under anesthesia. After euthanasia, mouse brains were removed. The brain samples were subsequently fixed for 48 hat 4 °C, paraffin-embedded and coronally sliced with the thickness of 4 μm. Then, the slices were incubated with endogenous peroxidase blocking buffer for 10 min at 25 °C. After incubation, the slices were blocked in goat serum for 30 min at 25 °C. Then, the slices were incubated with anti-tyrosine hydroxylase (TH), anti-ionized calcium-binding adapter molecule 1 (Iba-1) and anti-tumor necrosis factor-α (TNF-α) primary antibodies in an immunohistochemical wet box at 4 °C overnight [20].

After washes, the slices were subsequently incubated with secondary antibody for 20 min at 37 °C. After developing with 3, 3'-diaminobenzidine tertrahydrochloride (DAB) and counterstaining, the slices were scanned with a digital slide scanner (WS-10, Wisleap, Changzhou, Jiangsu, China). For quantitative analysis, the number of positive cells within the substantia nigra pars compacta (SNpc) region was measured in 4 individual 10× photomicrographs for each group.

2.16. Statistical Analysis

Statistical data were shown as means ± SEM from at least 3 independent experiments. Two-tailed Student's *t*-test for two group comparisons or one-way analysis of variance (ANOVA) with Bonferroni's test for multiple comparisons was performed using GraphPad Prism 6.0 software, and $P < 0.05$ was considered as statistically significant.

3. Results

3.1. ELE Alleviated Motor Impairment and Neuronal Damage in MPTP- Induced PD Mice

We first investigated the protective effects of ELE on MPTP-induced deficit of motor functions. Rotarod test showed that the PD model group mice had shorter retention time (76.60 ± 26.53 s) on the rotating rod compared to control group (168.8 ± 11.2 s), while ELE treatment (100 and 400 mg/kg) showed markable improvement in rotarod activity (139.0 ± 21.8 s and 167.4 ± 12.6 s, respectively) (Figure 1A). Pole test revealed that MPTP injection increased the time for mice to climb down the pole (9.800 ± 1.356 s) compared with control group (4.200 ± 0.374 s). However, the time was obviously shortened after ELE treatment (4.800 ± 0.800 s and 4.000 ± 0.632 s) (Figure 1B). Grip strength was also significantly increased in the ELE treatment group (249.9 ± 17.3 g and 291.4 ± 6.4 g, respectively) compared with PD model group (153.3 ± 6.9 g) (Figure 1C). Furthermore, gait analysis showed that PD mice responded to MPTP toxicity by decreasing speed and taking shorter strides and fewer normal step sequence. However, these parameters were significantly restored by ELE treatment, respectively (Figure 1D, 1E and 1F). Next, we detected the effect of ELE on TH positive dopaminergic neurons in SNpc. IHC analysis showed that MPTP administration induced a dramatic reduction of TH positive neurons in SNpc, which was effectively rescued by ELE (Figure 1G). Nissl staining showed that MPTP induced the decrease of Nissl substance and the shortening or loss of synapses in PD mice. However, ELE was still able to markedly restore the injury (Figure 1H). Collectively, these findings indicated that ELE protected motor performance impairment and neuronal damage in MPTP-induced PD mice in a dose-dependent manner.

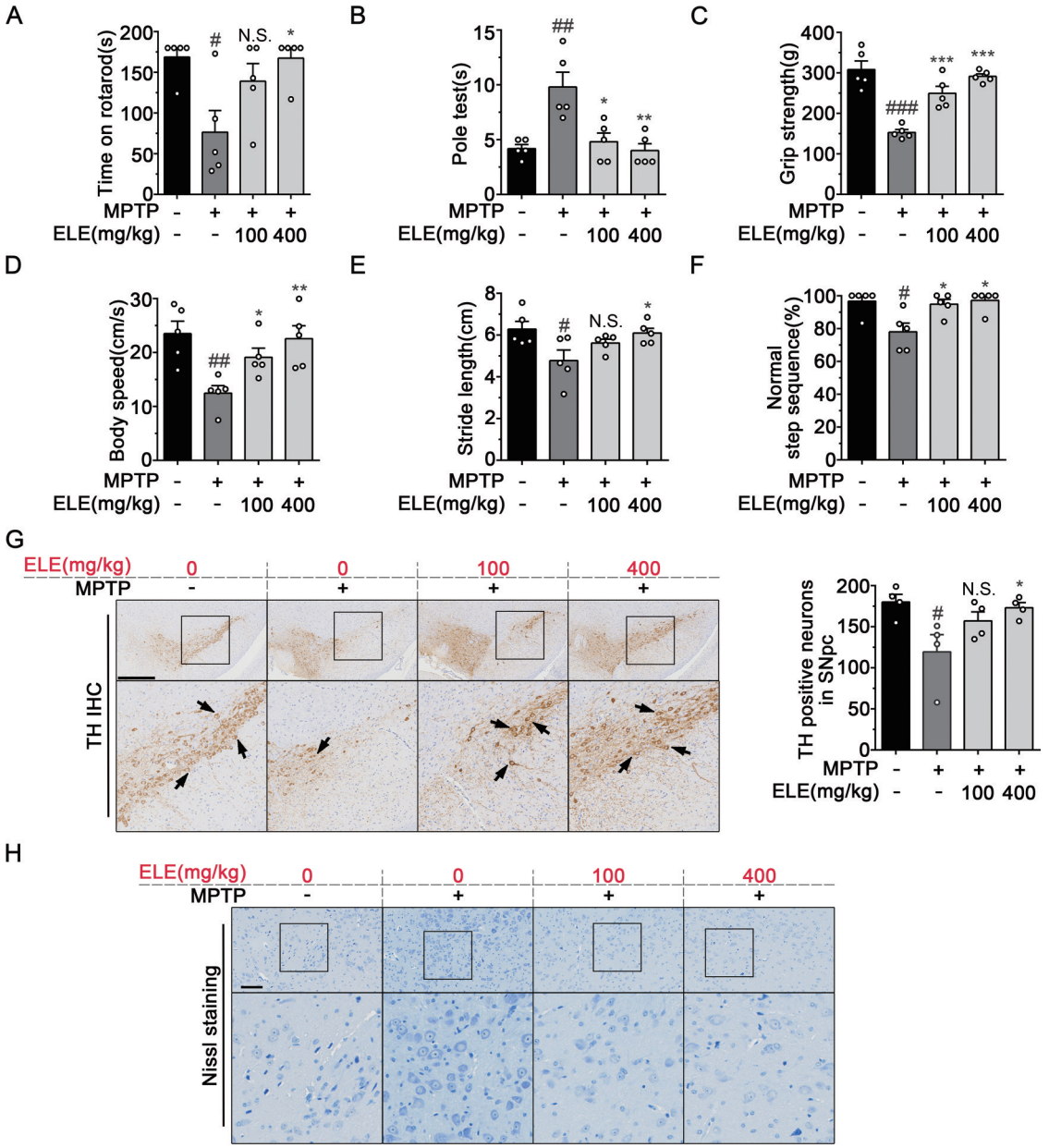

Figure 1. ELE alleviated motor impairment and neuronal damage in MPTP- induced PD mice. (**A, B, C**) Behavior analysis (rotarod test, pole test, and grip strength test) performed on the 5th day of MPTP injection indicated that ELE protected against motor deficits in MPTP-induced PD mice (n = 5). (**D, E, F**) Gait analysis performed on the 5th day of MPTP injection indicated that ELE alleviated gait variation in MPTP-induced PD mice. Parameters included speed, stride length and normal step sequence (n = 5). (**G**) IHC staining of TH in the SNpc region revealed that ELE rescued the loss of TH positive neurons. Arrowheads indicated positive expression of TH, scale bar = 500 μm. (**H**) Nissl. staining performed in the SNpc region revealed that ELE restored the MPTP- induced neuronal injury. Scale bar = 100 μm. Data were expressed as mean ± SEM for 4–5 individual experiments. $^{\#}P < 0.05$, $^{\#\#}P < 0.01$, $^{\#\#\#}P < 0.001$ vs control group, $^{*}P < 0.05$, $^{**}P < 0.01$, $^{***}P < 0.001$ vs PD model group.

3.2. ELE Inhibited Microglia-mediated Neuroinflammation in SNpc of MPTP-induced PD Mice

As abnormal activation of microglia and chronic neuroinflammation are common pathological features of PD [23], the number of Iba1 positive cells in SNpc was investigated by IHC. As shown in Figure 2A, Iba-1 positive cells in SNpc increased after MPTP injection. However, ELE markedly suppressed microglial activation as evidenced by decreased Iba-1 positive cells. Next, we tested the effect of ELE on the generation of pro-inflammatory cytokine TNF-α in SNpc. IHC analysis showed that MPTP radically promoted TNF-α

production in the SNpc region, which was reversed by ELE treatment (Figure 2B). Furthermore, the increased levels of iNOS and COX-2 in brain tissues derived from PD mice were obviously suppressed in response to ELE administration (Figure 2C). Collectively, these results suggested that ELE alleviated microglial activation and inhibited neuroinflammation in SNpc region of MPTP-induced PD mice.

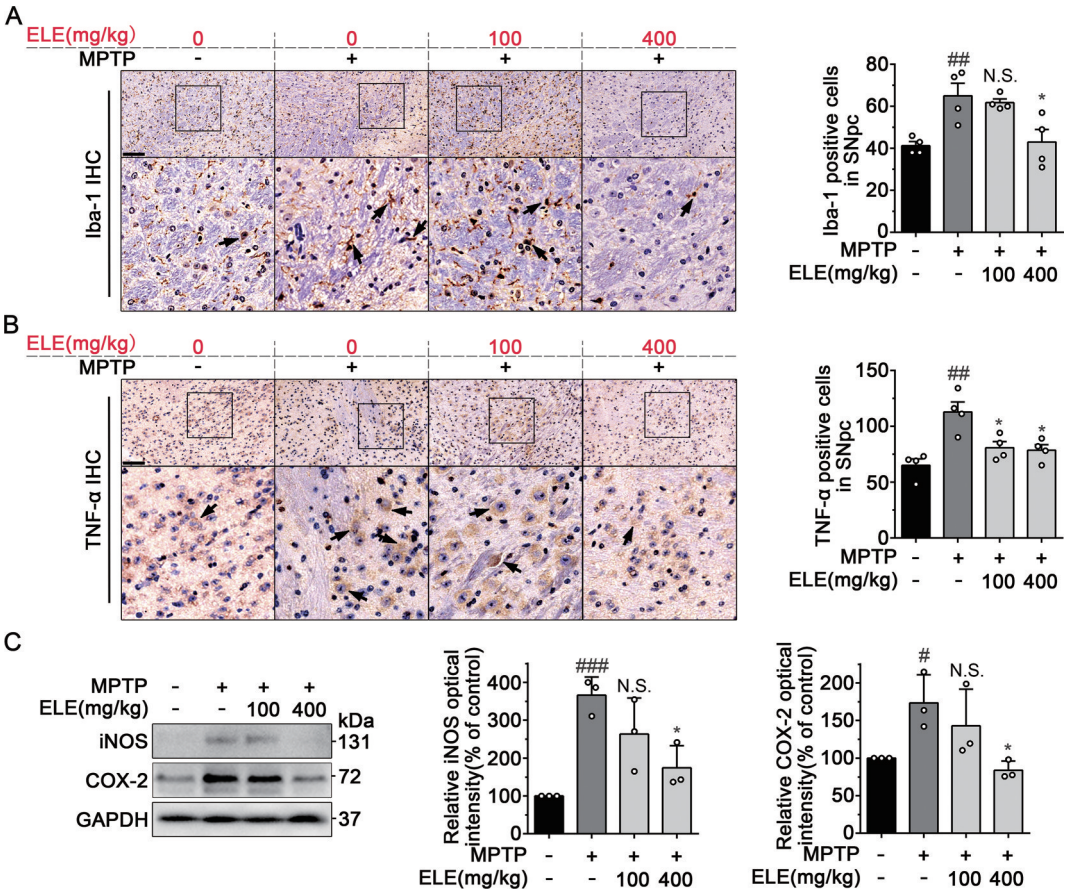

Figure 2. ELE inhibited microglia-mediated neuroinflammation in SNpc of MPTP-induced PD mice. (**A**) IHC staining of Iba1 in the SNpc region revealed that ELE reduced microglial activation. Arrowheads indicated the Iba1-positive microglia, scale bar = 100 μm. (**B**) IHC staining of TNF-α in the SNpc region indicated that ELE inhibited the generation of pro-inflammatory cytokine TNF- α . Arrowheads indicated positive expression of TNF-α, scale bar = 100 μm. (**C**) ELE downregulated the expression of iNOS and COX-2 in brain tissues of MPTP-induced PD mice. Data were expressed as mean ± SEM for 3–4 individual experiments. $^{\#}P < 0.05$, $^{\#\#}P < 0.01$, $^{\#\#\#}P < 0.001$ vs control group, $^{*}P < 0.05$ vs PD model group.

3.3. ELE Suppressed LPS-Induced Inflammation in BV-2 Cells and Protected Neuronal Injury

We further confirmed the anti-neuroinflammatory effect of ELE in vitro with LPS-induced BV-2 cells. In our previous experiment, we explored the optimum concentration of ELE to inhibit neuroinflammation. The results showed that the NO production was slightly suppressed with ELE treatment in 6.25 μg/mL, while ELE treatment above 50 μg/mL completely suppressed NO release. Therefore, we chose the optimum concentration of 12.5, 25 and 50 μg/mL ELE to research the inhibition of neuroinflammation. ELE significantly inhibited the release of NO against LPS stimulation in BV-2 cells in 12.5, 25, and 50 μg/mL (Figure 3A). Besides, MTT assay showed that ELE had no effect on the survival of BV-2 cells (Figure 3B). We also confirmed that ELE obviously inhibited BV-2 microglial activation by down-regulating pro-inflammatory factors including IL-6 and TNF-α in a concentration-dependent manner (Figure 3C and 3D). Meanwhile, ELE suppressed the expressions of iNOS and COX-2 in LPS- induced BV-2 cells (Figure 3E), indicating a notable anti-neuroinflammatory effect. Since ELE had shown inhibitory effects on excessive activation of microglia, we tried to explore whether it could alleviate the neurotoxic effects of activated

microglia on neurons. To address this issue, we identified the toxicity of LPS-stimulated BV-2 microglial cell-conditioned medium (CM) to PC12 cells (Figure 3F). As a result, PC12 cell death was observed upon exposure to CM from LPS-stimulated BV-2 cells (Figure 3G). However, treatment with ELE appreciably decreased the toxicity of CM and rescued PC12 cells damage (Figure 3G). Crystal violet staining assays showed that ELE ameliorated the morphological changes of PC12 cells and reduced the cell death after CM-mediated damage (Figure 3H). Taken together, these data suggested that ELE inhibited LPS-induced inflammation in BV-2 cells and suppressed microglia- mediated neuronal damage.

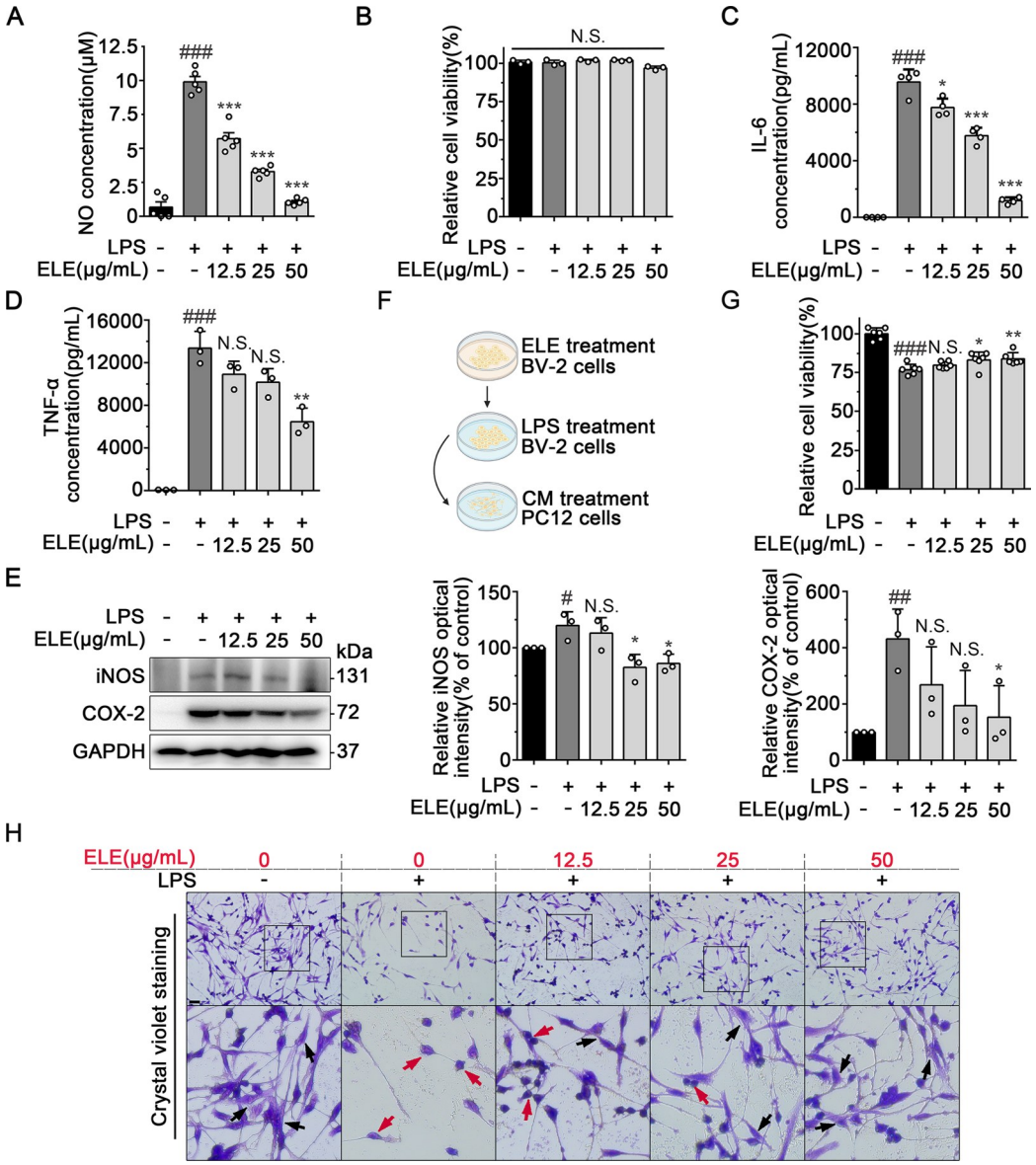

Figure 3. ELE suppressed LPS-induced inflammation in BV-2 cells and thus protected neuronal injury. (**A**) ELE suppressed LPS-induced NO release in BV- 2 cells. (**B**) MTT analysis showed that ELE had no effect on BV-2 cells viability. (**C** and **D**) ELISA analysis showed that ELE decreased the release of IL-6 and TNF-α from LPS-induced BV-2 cells. (**E**) ELE inhibited the expression of iNOS and COX-2 in LPS-induced BV-2 cells. BV-2 cells were treated with LPS (1 μg/mL) with different concentrations of ELE (12.5, 25, and 50 μg/mL) for 24 h for western blot analysis. (**F**) Schematic diagram of the PC12 cells culture treated with CM. Biorender was used to create the schematic diagram. (**G**) MTT. analysis showed that ELE ameliorated the effect of CM on PC12 cells survival. (**H**) Crystal violet staining assay indicated that ELE protected PC12 cells morphology and maintained the cell number. Black arrowheads indicated normal PC12 cells, red arrowheads indicated damaged PC12 cells. Data were expressed as mean ± SEM for 3−6 individual experiments. $^{\#}P < 0.05$, $^{\#\#}P < 0.01$, $^{\#\#\#}P < 0.001$ vs control group, $^{*}P < 0.05$, $^{**}P < 0.01$, $^{***}P < 0.001$ vs LPS-induced group.

3.4. Cellular Target Proteins Identification of ELE via Affinity Purification

Cellular target identification is crucial to explore the pharmacological mechanisms [19,24]. To explore the potential target proteins of ELE, we prepared ELE-crosslinked nanoparticles (ELE beads) to capture direct target proteins from BV-2 cell lysates using affinity purification-mass spectrometry-based proteomics strategy (Figure 4A). As shown in Figure 4B, we discovered 926 proteins in total. Further, 305 differentially abundant proteins were identified (*P*-value < 0.05 and the protein fold change > 1.5) for ELE-binding (Figure 4B). Subsequently, the 305 potential target proteins were investigated by KEGG pathway analysis, and the significant signaling pathways were obtained. Since imbalances of energy is highly associated with inflammation progress [25–27], we then focused on the major energy-sensing AMP-activated protein kinase (AMPK) signaling pathway for further study (Figure 4C). The Parkinson's disease-related protein network was also enriched by KEGG analysis, consistent with the anti-PD activity of ELE.

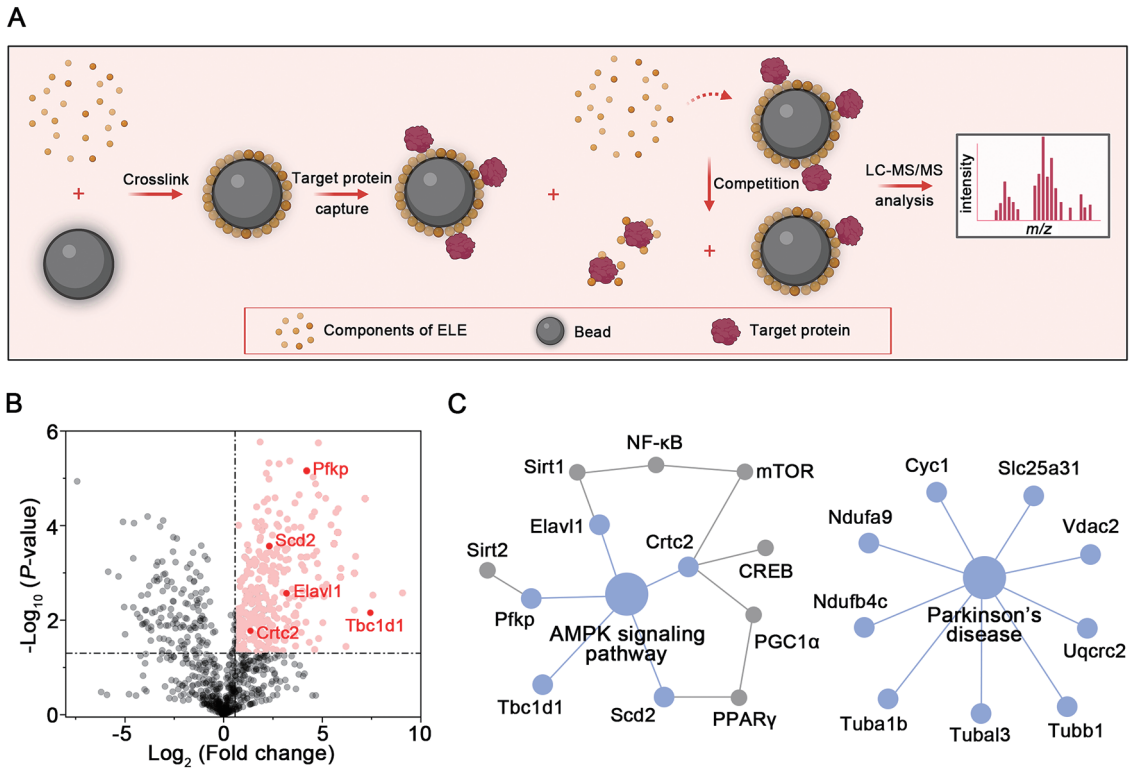

Figure 4. Cellular target proteins identification of ELE via affinity purification. (**A**) Schematic diagram of pull-down/MS-based target identification of ELE. Biorender was used to create the schematic diagram. (**B**) Volcano plot showed the target profiles of ELE. A protein fold change of > 1.5 implied abundant proteins. A *P*-value of < 0.05 indicated statistical significance. (**C**) AMPK signaling pathway and Parkinson's disease-related protein network was enriched by KEGG analysis.

3.5. ELE Exerted Anti-Neuroinflammation Effect through Regulating AMPK/mTOR/NF-κB Pathway

AMPK is a key regulator of cellular energy homeostasis in eukaryotes [28]. The activation of AMPK has been reported to exert anti-inflammatory effects, and mTOR acts as a downstream effector of AMPK signaling [29,30]. Here, we put special focus on the AMPK/mTOR signaling pathway to investigate the anti-neuroinflammatory mechanisms of ELE on LPS-induced BV-2 cells. As shown in Figure 5A, ELE obviously increased the level of phosphorylated AMPK and inhibited phosphorylation of mTOR compared with LPS-induced BV-2 cells, indicating that ELE activated AMPK/mTOR signaling pathway in BV-2 cells. Accumulating experimental evidence reveals that AMPK reduces inflammatory processes by inhibiting NF-κB activity [31]. Thus, activation of AMPK/mTOR signaling contributes to negative regulation of NF-κB signaling pathway, thereby blocking microglial activation [29,32]. Our results indicated that ELE obviously

inhibited LPS-mediated activation of IκB kinase (IKK)-β. The reduced IKK-β activity led to downregulation of phosphorylation level of inhibitor of NF-κB (IκB). Furthermore, inhibition of IκB phosphorylation suppressed NF-κB p65 activation, thus inhibiting NF-κB signaling pathway (Figure 5B). Conclusively, ELE suppressed LPS-induced neuroinflammation by regulating the AMPK/mTOR/NF-κB pathway in BV-2 cells.

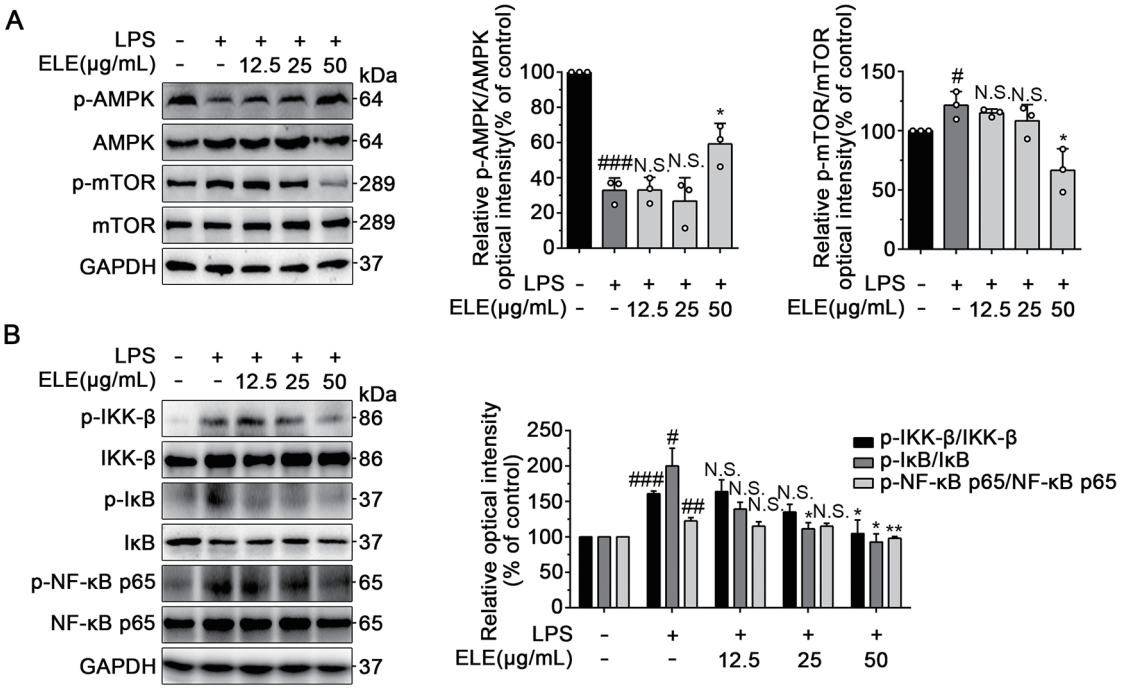

Figure 5. ELE exerted anti-neuroinflammation effect through regulating AMPK/mTOR/NF-κB pathway. (**A**) ELE activated the activity of AMPK/mTOR signaling pathway. BV-2 cells were treated with LPS (1 μg/mL) with different concentrations of ELE (12.5, 25, and 50 μg/mL) for 12 h for western blot analysis. (**B**) ELE inhibited LPS-mediated activation of the NF-κB signaling pathway. BV-2 cells were treated with LPS (1 μg/mL) with different concentrations of ELE (12.5, 25, and 50 μg/mL) for 10 min for p-IKK-β/ IKK-β, 30 min for p-IκB/ IκB, and 1 h for p-NF-κB p65/ NF-κB p65 for western blot analysis. Data were expressed as mean ± SEM for 3 individual experiments. $^{\#}P < 0.05$, $^{\#\#}P < 0.01$, $^{\#\#\#}P < 0.001$ vs control group, $^{*}P < 0.05$, $^{**}P < 0.01$ vs LPS-induced group.

4. Discussion

Based on accumulating evidence, microglial activation-mediated neuroinflammation is one of the most important pathogenic factors in the etiology of PD [10,33,34]. However, drugs targeting microglial activation as a therapeutic approach in PD are still lacking [35]. *Eupatorium lindleyanum* has been reported to possess a wide range of pharmacological properties, such as reducing phlegm, suppressing cough, and relieving asthma [16,36,37]. In the present work, we indicated that ELE exerted protective effects on MPTP- induced PD mice. Moreover, ELE notably inhibited microglial activation in SNpc of PD mice. In mechanisms, ELE markedly reduced the contents of NO, IL-6, and TNF-α in LPS-induced BV-2 cells, indicating that the neuroprotective effect of ELE in PD may be closely associated with the anti-neuroinflammatory activity.

ELE protected against neuronal damage and inhibited the progression of PD pathology via targeting neuroinflammation. Therefore, ELE provided a neuroprotective effect in MPTP-induced PD by suppressing the activation of microglia as well as neuroinflammation. Furthermore, the neuroprotective mechanisms of ELE were likely to extend beyond its anti-neuroinflammatory properties, encompassing antioxidant, anti-apoptotic, and neurotrophic effects. Further research is needed to confirm the precise mechanisms underlying the neuroprotective effects of ELE on PD.

Traditional herbal medicines play a critical role in the treatment of complicated diseases [38–40]. As a multi-molecule system, the medicinal plant extract has a wide range of medicine properties [41,42]. However,

their multi- target mechanisms of action remains to be clarified [19,41]. In this study, we utilized an affinity purification-based cellular target identification technology (previously reported as ZY strategy), which was developed by our lab [19], and identified 305 potential target proteins of ELE. Briefly, complex compounds from ELE were photochemically crosslinked onto the surface of nanoparticles, thereby generating ELE beads for capturing target proteins from BV-2 cell lysates. This strategy is identical to the characteristics of multi-molecule systems that exhibit pharmacological activities through modulating multiple target proteins. The results also indicated that ELE exerted anti-PD effects via modulating multiple targets.

The bioinformatics analysis was based on the identified targets and indicated that ELE treatment had an influence on the AMPK signaling pathway. The potential role of AMPK is served as a cellular energy sensor, while mTOR plays a vital role in cell metabolism as well as inflammation processes [43,44]. Activation of AMPK is known to decrease mTOR activity, which further inhibits IKK/NF-κB activation [31,45]. In this study, we found that ELE activated AMPK and inhibited mTOR signaling in LPS-induced BV-2 cells. Meanwhile, ELE inhibited LPS-mediated activation of the NF-κB signaling pathway. Therefore, ELE may exert anti-neuroinflammatory activity via targeting AMPK/mTOR/NF- κB pathway. The intricate mechanisms highlighted the potential of ELE as a therapeutic agent for suppressing neuroinflammation in PD.

The study of the therapeutic effect of natural compounds on PD models has attracted widespread attention. Many studies have shown that some natural compounds have antioxidant, anti-inflammatory, and neuroprotective properties, which may be important for the treatment of PD. For example, some natural products such as resveratrol, gastrodin and tanshinone have been found to protect neuron cells from damage by reducing oxidative stress and inhibiting inflammatory responses [46]. In addition, certain natural products such as icariin and saffron flavonoid extract have also shown potential therapeutic effects on PD [47]. However, it should be noted that further research is needed to verify the safety and efficacy of natural products before applying them to clinical practice. As a kind of natural product, ELE exerts anti-PD activity through its anti-inflammatory effects. We hope the present research on ELE can contribute to new studies on the mechanisms and treatment methods of PD.

Taken together, the present study provides a new insight into the mechanisms of ELE against PD. Furthermore, the results also reflect the multicomponent and multitarget characteristics of natural-derived plant extracts.

5. Conclusion

EL has the functions of suppressing cough and resolving phlegm. However, the anti-PD activity of EL has not been investigated until now. Our results reveal that ELE significantly inhibit PD pathological process via multiple targets- mediated anti-neuroinflammatory mechanisms. ELE alleviated motor impairment and neuronal damage in MPTP-induced PD mice. Furthermore, ELE notably suppressed microglial activation in SNpc of PD mice. In mechanisms, ELE dose-dependently inhibited LPS-induced BV-2 microglial activation via AMPK/mTOR/NF-κB signaling pathway. These findings indicate that ELE may represent a promising therapeutic agent for PD.

Abbreviations: AMPK: AMP-activated protein kinase; ANOVA, analysis of variance; BCA, bicinchoninic acid; CM, conditioned medium; COX-2, cyclooxygenase-2; DA, dopamine; DHBP, 4, 4'-dihydroxybenzophenone; DAB, 3, 3'-diaminobenzidine tertrahydrochloride; DMEM, dulbecco's modified eagle medium; DMSO, dimethyl sulfoxide; EB, eupalinolide B; ECL, enhanced chemiluminescence; EL, *Eupatorium lindleyanum* DC.; ELE, EL extract; Iba-1, ionized calcium-binding adapter molecule 1; IHC, immunohistochemical; IKK, IκB kinase; IκB, inhibitor of NF-κB; Il-6, interleukin-6; ELISA, enzyme-linked immunosorbent assay; FBS, fetal bovine serum; HRP, horseradish peroxidase; iNOS, inducible nitric oxide synthase; KEGG, kyoto encyclopedia of genes and genomes; LPS, lipopolysaccharide; MPTP, 1-methyl-4-phenyl-1, 2, 3, 6-tetrahydropyridine; mTOR, mammalian target of rapamycin; MTT, 3- (4, 5) -dimethylthiahiazo(-z-y1) -3, 5-di-phenytetrazoliumromide; NF- κB, nuclear factor- κB; NO, nitric oxide; NPs, nanoparticles; PBS, phosphate buffered saline; PD, Parkinson's disease; PMSF, phenylmethylsulfonylfluoride; PVDF, polyvinylidene fluoride; RIPA, radio immunoprecipitation assay lysis buffer; SDS-PAGE, sodium dodecyl-sulfate polyacrylamide gel electrophoresis; SNpc, substantia nigra pars compacta; TBST, Tris-buffered saline with Tween 20; TH, tyrosine hydroxylase; TNF-α, tumor necrosis factor-α .

Author Contributions: K.Z. conceived and supervised the project. Y.Z. did most of the pharmacologic experiments.L.Y., X.Z., Z.Y. and Y.Z. assisted in part of the biochemical experiments. L.Z., Y.C., W.Y., N.Z.M. and B.H.provided technical services. K.Z., Y.Z., R.F.M. and P.T. analyzed the data and wrote the manuscript.

Funding: This work was financially supported by National Key R&D Program of China (2022YFC3501601), Beijing Natural Science Foundation (7232273), Jinan New 20 Policies for Higher Education Funding (202228048), and the Special Fund for "Tian-Chi Talent Introduction Program".

Institutional Review Board Statement: Not applicable.

Informed Consent Statement: Not applicable.

Data Availability Statement: Not applicable.

Conflicts of Interest: There are no conflicts of interest to declare.

References

1. Panicker, N.; Kam, T.I.; Wang, H.; et al. Neuronal NLRP3 is a parkin substrate that drives neurodegeneration in Parkinson's disease. *Neuron*. **2022**, *110*, 2422–2437.
2. Gordon, R.; Albornoz, E.A.; Christie, D.C.; et al. Inflammasome inhibition prevents α-synuclein pathology and dopaminergic neurodegeneration in mice. *Sci. Transl. Med.* **2018**, *10*, eaah4066, https://doi.org/10.1126/scitranslmed.aah4066.
3. Qian, H.; Kang, X.; Hu, J.; et al. Reversing a model of Parkinson's disease with in situ converted nigral neurons. *Nature* **2020**, *582*, 550–556, https://doi.org/10.1038/s41586-020-2388-4.
4. Bloem, B.R.; Okun, M.S.; Klein, C. Parkinson's disease. The Lancet. **2021**, *397*, 2284–2303.
5. Qu, C.; Liu, L.; Xu, Q.Q. Neuroprotective effects of San-Jia-Fu-Mai decoction: Studies on the in vitro and in vivo models of Parkinson's disease. *World J. Tradit. Chin. Med*. **2021**, *7*, 192–200.
6. Raza, C.; Anjum, R.; Shakeel, N.U.A. Parkinson's disease: Mechanisms, translational models and management strategies. *Life Sci.* **2019**, *226*, 77–90, https://doi.org/10.1016/j.lfs.2019.03.057.
7. Hirsch, E.C.; Hunot, S. Neuroinflammation in Parkinson's disease: a target for neuroprotection? *Lancet Neurol*. **2009**, *8*, 382–397.
8. Pajares, M.; Rojo, A.I.; Manda, G.; et al. Inflammation in Parkinson's Disease: Mechanisms and Therapeutic Implications. *Cells* **2020**, *9*, 1687, https://doi.org/10.3390/cells9071687.
9. Zhou, Q.; Le, M.L.; Yang, Y.Y. Discovery of novel phosphodiesterase-1 inhibitors for curing vascular dementia: Suppression of neuroinflammation by blocking NF-kappaB transcription regulation and activating cAMP/CREB axis. *Acta. Pharm. Sin. B*. **2023**, *13*, 1180–1191.
10. Kim, B.-W.; Koppula, S.; Park, S.-Y.; et al. Attenuation of neuroinflammatory responses and behavioral deficits by Ligusticum officinale (Makino) Kitag in stimulated microglia and MPTP-induced mouse model of Parkinson's disease. *J. Ethnopharmacol.* **2015**, *164*, 388–397, https://doi.org/10.1016/j.jep.2014.11.004.
11. Zhang, L.; Wang, Y.; Liu, T.; et al. Novel Microglia-based Therapeutic Approaches to Neurodegenerative Disorders. *Neurosci. Bull.* **2023**, *39*, 491–502, https://doi.org/10.1007/s12264-022-01013-6.
12. Huang, B.X.; Liu, J.X.; Meng, T.Y. Polydatin prevents lipopolysaccharide (LPS)- induced Parkinson's disease via regulation of the AKT/GSK3β-Nrf2/NF-κB signaling axis. *Front. Immunol*. **2018**, *9*, 2527.
13. Chu, C.J.; Ren, H.L.; Xu, N.Y. *Eupatorium lindleyanum* DC. sesquiterpenes fraction attenuates lipopolysaccharide-induced acute lung injury in mice. *J. Ethnopharmacol*. **2016**, *185*, 263–271.
14. Huang, L.; Xu, D.Q.; Chen, Y.Y. Qualitative and quantitative analysis of chemical components in *Eupatorium lindleyanum* DC. by ultra-performance liquid chromatography-mass spectrometry integrated with anti-inflammatory activity research. *J. Sep. Sci.* **2021**, *44*, 3174–3187.
15. Chu, C.; Yao, S.; Chen, J.; et al. *Eupatorium lindleyanum* DC. flavonoids fraction attenuates lipopolysaccharide-induced acute lung injury in mice. *Int. Immunopharmacol.* **2016**, *39*, 23–33, https://doi.org/10.1016/j.intimp.2016.06.032.
16. Wang, X.; Ma, S.; Lai, F.; et al. Traditional Applications, Phytochemistry, and Pharmacological Activities of *Eupatorium lindleyanum* DC.: A Comprehensive Review. *Front. Pharmacol*. **2020**, *8*, 577124 https://doi.org/10.3389/fphar.2020.577124.
17. Zheng, S.Z.; Zhang, X.W.; Song, X.M.; et al. Epoxymicheliolide directly targets histone H2B to inhibit neuroinflammation via recruiting E3 ligase RNF20. *Pharmacol. Res.* **2022**, *177*, 106093, https://doi.org/10.1016/j.phrs.2022.106093.
18. Kong, X.; Ai, G.; Wang, D.; et al. PDE4 and Epac1 Synergistically Promote Rectal Carcinoma via the cAMP Pathway. *Anal. Cell. Pathol.* **2019**, *2019*, 1–5, https://doi.org/10.1155/2019/7145198.
19. Zhao, M.; Yao, L.; Zhang, X.; et al. Global identification of the cellular targets for a multi-molecule system by a photochemically-induced coupling reaction. *Chem. Commun.* **2021**, *57*, 3449–3452, https://doi.org/10.1039/d1cc00392e.
20. Zhang, X.W.; Feng, N.; Liu, Y.C.; et al. Neuroinflammation inhibition by small-molecule targeting USP7 noncatalytic domain for neurodegenerative disease therapy. *Sci. Adv.* **2022**, *8*, eabo0789, https://doi.org/10.1126/sciadv.abo0789.
21. Zheng, Z.V.; Cheung, C.Y.; Lyu, H.; et al. Baicalein enhances the effect of low dose Levodopa on the gait deficits and protects dopaminergic neurons in experimental Parkinsonism. *J. Clin. Neurosci.* **2019**, *64*, 242–251, https://doi.org/10.1016/j.jocn.2019.02.005.
22. Wang, X.H.; Lu, G.; Hu, X.; et al. Quantitative assessment of gait and neurochemical correlation in a classical murine model of Parkinson's disease. *BMC Neurosci.* **2012**, *13*, 142–142, https://doi.org/10.1186/1471-2202-13-142.

23. Li, Y. N.; Xia, Y.; Yin, S. J. Targeting microglial α-synuclein/TLRs/NF- kappaB/NLRP3 inflammasome axis in Parkinson's disease. *Front. Immunol.* **2021**, *12*, 719807.
24. Yao, L.; Liao, M.; Wang, J. K.; et al. Gold Nanoparticle-Based Photo-Cross-Linking Strategy for Cellular Target Identification of Supercomplex Molecular Systems. *Anal. Chem.* **2022**, *94*, 3180–3187, https://doi.org/10.1021/acs.analchem.1c04652.
25. Zhao, G.; He, F.; Wu, C.; et al. Betaine in inflammation: Mechanistic Aspects and Applications. *Front. Immunol.* **2018**, *9*, 1070, https://doi.org/10.3389/fimmu.2018.01070.
26. Hernandez-Baixauli, J.; Abasolo, N.; Palacios-Jordan, H.; et al. Imbalances in TCA, Short Fatty Acids and One-Carbon Metabolisms as Important Features of Homeostatic Disruption Evidenced by a Multi-Omics Integrative Approach of LPS-Induced Chronic Inflammation in Male Wistar Rats. *Int. J. Mol. Sci.* **2022**, *23*, 2563, https://doi.org/10.3390/ijms23052563.
27. Behl, T.; Kumar, S.; Singh, S.; et al. Reviving the mutual impact of SARS-COV-2 and obesity on patients: From morbidity to mortality. *Biomed. Pharmacother.* **2022**, *151*, 113178–113178, https://doi.org/10.1016/j.biopha.2022.113178.
28. Hardie, D. G.; Schaffer, B. E.; Brunet, A. AMPK: An Energy-Sensing Pathway with Multiple Inputs and Outputs. *Trends Cell Biol.* **2015**, *26*, 190–201, https://doi.org/10.1016/j.tcb.2015.10.013.
29. Chen, Y. H.; Li, Y. P.; Li, C. X. Dexmedetomidine alleviates pain in MPTP-treated mice by activating the AMPK/mTOR/NF-kappaB pathways in astrocytes. *Neurosci. Lett*. **2022**, *791*, 136933.
30. Kim, D. Y.; Leem, Y. H.; Park, J. S.; et al. RIPK1 Regulates Microglial Activation in Lipopolysaccharide-Induced Neuroinflammation and MPTP-Induced Parkinson's Disease Mouse Models. *Cells* **2023**, *12*, 417, https://doi.org/10.3390/cells12030417.
31. Han, C.J.; Zheng, J.Y.; Sun, L. The oncometabolite 2-hydroxyglutarate inhibits microglial activation via the AMPK/mTOR/NF-kappaB pathway. *Acta. Pharmacol. Sin*. **2019**, *40*, 1292–1302.
32. Yu, Q.; Zeng, K.W.; Ma, X.L.; et al. Ginsenoside Rk1 suppresses pro-inflammatory responses in lipopolysaccharide-stimulated RAW264.7 cells by inhibiting the Jak2/Stat3 pathway. *Chin. J. Nat. Med.* **2017**, *15*, 751–757, https://doi.org/10.1016/s1875-5364(17)30106-1.
33. Herrero, M. T.; Estrada, C.; Maatouk, L. Inflammation in Parkinson's disease: role of glucocorticoids. *Front. Neuroanat.* **2015**, *9*, 32.
34. Gan, P.; Xia, Q. F.; Hang, G. H. Knockdown of cathepsin D protects dopaminergic neurons against neuroinflammation-mediated neurotoxicity through inhibition of NF-κB signalling pathway in Parkinson's disease model. *Clin. Exp. Pharmacol. Physiol*. **2019**, *46*, 337–349.
35. Chen, Y. H.; Jiang, M. J.; Li, L. DL-3-n-butylphthalide reduces microglial activation in lipopolysaccharide-induced Parkinson's disease model mice. *Mol. Med. Rep.* **2018**, *17*, 3884–3890.
36. Zhang, Y.; Dong, F.; Cao, Z.; et al. Eupalinolide A induces autophagy via the ROS/ERK signaling pathway in hepatocellular carcinoma cells *in vitro* and *in vivo*. *Int. J. Oncol.* **2022**, *61*, 1–16, https://doi.org/10.3892/ijo.2022.5421.
37. Wang, F.; Zhong, H. H.; Fang, S. Q. Potential anti-inflammatory sesquiterpene lactones from Eupatorium lindleyanum. *Planta. Med.* **2018**, *84*, 123–128.
38. Lv, H. N.; Wen, R.; Zhou, Y.; et al. Nitrogen Oxide Inhibitory Trimeric and Dimeric Carbazole Alkaloids from *Murraya tetramera*. *J. Nat. Prod.* **2015**, *78*, 2432–2439, https://doi.org/10.1021/acs.jnatprod.5b00527.
39. Liu, B. Y.; Zhang, C.; Zeng, K. W.; et al. Anti-Inflammatory Prenylated Phenylpropenols and Coumarin Derivatives from *Murraya exotica*. *J. Nat. Prod.* **2018**, *81*, 22–33, https://doi.org/10.1021/acs.jnatprod.7b00518.
40. Zhang, J.; Hu, K.; Di, L.; et al. Traditional herbal medicine and nanomedicine: Converging disciplines to improve therapeutic efficacy and human health. *Adv. Drug Deliv. Rev.* **2021**, *178*, *113964*, https://doi.org/10.1016/j.addr.2021.113964.
41. Peng, X.; Tang, F.; Yang, Y.; et al. Bidirectional effects and mechanisms of traditional Chinese medicine. *J. Ethnopharmacol.* **2022**, *298*, 115578, https://doi.org/10.1016/j.jep.2022.115578.
42. Yang, Y.; Wu, C. The linkage of gut microbiota and the property theory of traditional Chinese medicine (TCM): Cold-natured and sweet-flavored TCMs as an example. *J. Ethnopharmacol.* **2023**, *306*, 116167, https://doi.org/10.1016/j.jep.2023.116167.
43. Steinberg, G. R.; Hardie, D. G. New insights into activation and function of the AMPK. *Nat. Rev. Mol. Cell Biol.* **2023**, *24*, 255–272, https://doi.org/10.1038/s41580-022-00547-x.
44. Mao, B.; Zhang, Q.; Ma, L.; et al. Overview of Research into mTOR Inhibitors. *Molecules* **2022**, *27*, 5295, https://doi.org/10.3390/molecules27165295.
45. Ding, Y. J.; Peng, Y. M.; Wu, H. L. The protective roles of liraglutide on Kawasaki disease via AMPK/mTOR/NF-kappaB pathway. *Int. Immunopharmacol.* **2023**, *117*, 110028.
46. Fu, Y.; Yang, J.; Wang, X.; et al. Herbal Compounds Play a Role in Neuroprotection through the Inhibition of Microglial Activation. *J. Immunol. Res.* **2018**, *2018*, 1–8, https://doi.org/10.1155/2018/9348046.
47. Qiao, J.; Wang, C.; Chen, Y.; et al. Herbal/Natural Compounds Resist Hallmarks of Brain Aging: From Molecular Mechanisms to Therapeutic Strategies. *Antioxidants* **2023**, *12*, 920, https://doi.org/10.3390/antiox12040920.